Tadulako Science and Technology Journal
Vol 1, No. 2, 2021, pp. 1-8
e-ISSN 2776-4893

Subsurface Fault Geometry Model Based on Type Resistance Data (Laboratory Scale Review)

M. F. W. Yanto [a,1)*] , M. R. Muin [a,2] , Moh. Dahlan Th. Musa [a,3], M. Rusydi. H [a,4] , Sandra [a,5] Badaruddin [a,6]

[a] Department of Geophysics Faculty of Mathematics and Natural Sciences Tadulako University, Jl. Soekarna Hatta, Palu, 94118, Indonesia
[1] fajarwidjayanto051@gmail.com
* corresponding author

ARTICLE INFO

Keywords
Geoelectri
Model
Wenner

ABSTRACT

Introduction: Research has been carried out with the title "Geometry of Fault Model Subsurface Based on Resistivity Data (Laboratory case)" with the aim of testing the effectiveness of the geoelectric method for identifying the geometry and direction of fault alignment, as well as knowing the geometry and direction of fault alignment based on resistivity data. **Method**: This research uses the Wenner configuration with azimuthal measurement techniques, totaling 24 electrode measurements. Data processing uses Res2dinv software release 3.53. **Results and Discussion**: The results obtained show the effectiveness of the geoelectric method in identifying fault-type obstacles, it is more appropriate to carry out measurements in parallel and perpendicular directions of the fault model. **Conclusion**: Then the fault geometry model obtained shows that the normal fault model has a resistivity value of 309 - 2254.26 Ωm and the thrust fault model has a resistivity value of 100 - 467.26 Ωm which is the resistivity value of granite, where this layer is a model of the fault.

1. Introduction

Regionally, Sulawesi Island has a complex tectonic setting, especially in the Palu Basin and surrounding areas. This region is traversed by a geological structure in the form of the active Palu-Koro fault which is the primary fault [7]. The Palu-Koro fault is found extending approximately 250 km in an almost north-south direction starting from Donggala at the end of Palu Bay to Bone Bay [2]. In addition to the primary fault, there are also secondary faults that form a flower structure [7].

A fault is a fracture plane accompanied by a relative shift (displacement) between one block and another rock block [4]. Fault research and identification are very important for earthquake-resistant building infrastructure planning [1]. Laboratory-scale research can provide better knowledge of the existence of faults to complement existing information. Research on complex geological structures in the field can be modeled on a laboratory scale [9].

The specific resistance geoelectric method is one of the techniques that can be used for recognizing the presence of faults in the subsurface [14]. Wahyuni conducted laboratory-scale geoelectric measurements to identify tilted layers and compared them with the shadow (analytical) method. The results show the value of apparent type resistance between analytical and experimental methods, namely the Wenner configuration has an error of 12.7% and the Schlumberger configuration has an error of 24.4%. Subiyanto (2010) also conducted laboratory-scale geoelectric measurements to identify subsurface faults.

The results of his research show that faults are represented by a shift in the value of the specific resistance between rock layers so that the slope that occurs in the rock layer can be displayed [18]. Ramdani also used geoelectric methods to analyze the pattern of apparent specific resistance due to faults in the subsurface through physical modeling in the laboratory. The measurement technique used is 1D Azimut Resistivity Survey (ARS). The results of his research show that the pseudo-type resistance pattern can show the direction of the fault as an anomalous object well [10].

In this thesis research, the geoelectric method of specific resistance will be used to identify the geometry of subsurface faults. The test will be conducted on a laboratory scale by modeling a fault replica immersed in a soil box. The technique to be used is Azimut Resistivity Survey (ARS) with Wenner configuration. Based on the contrast of the specific resistance values, it is expected to get an idea of the geometry model and the direction of the fault alignment.

The specific resistance geoelectric method is one of the geoelectric techniques that focuses on researching the characteristics of the specific resistance of rock layers in the earth. The basic principle of this method is to conduct an electric current into the ground through a pair of current electrodes, while the potential difference that occurs is measured through a pair of potential electrodes. From the measurement data of current and electric potential differences, we can determine the variation of the specific resistance value of the layer below the measurement point [14]. This geoelectric method is often used as an exploration technique, especially in the study of subsurface faults and geological structures. The arrangement of current electrodes and potential electrodes in the measurement of the geoelectric method of specific resistance can be seen in Figure 1.

The Automatic Array Scanning (AAS) method is one of the measurement techniques in the type resistance geoelectric method. In the AAS method, measurements are taken repeatedly and sequentially using a specified depth penetration. Initially, Barker (1981) conducted research using the Offset Wenner method. Later, Van Overmeeren and Ritsema (1988) named this method Continous Vertical Electrical Sounding (CVES) and applied it in hydrological studies. This method is also known as Electrical Resistivity Tomography (ERT). ERT is a multi-electrode geo-electrical method used to obtain information about the condition of materials under the earth's surface based on the distribution pattern of the material's type resistance value [11].

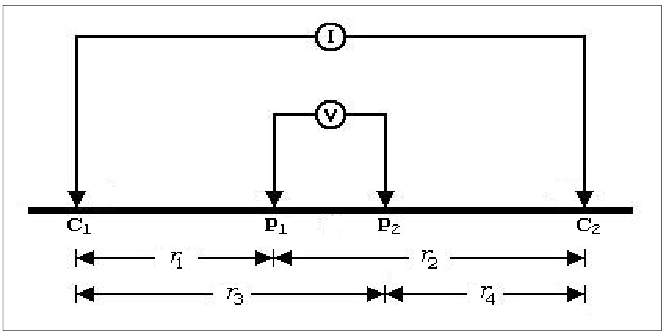

Fig 1. Wenner Configuration Electrode Array

ARS is a measurement technique used to measure specific resistance using the Wenner configuration by rotating the direction of the measurement trajectory by a certain angle [10]. Changes in the value of the specific resistance based on directional variations are used in analyzing the structure of the subsurface geology. Anisotropy is the difference in properties and parameters of a medium in different directions. The ARS measurement technique is illustrated in Figure 2.6 below.

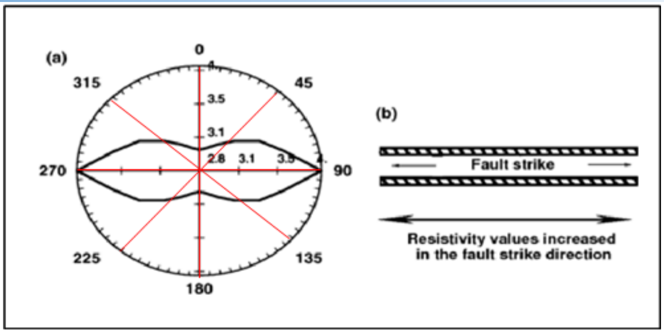

Fig 2. (A) ARS Technique With 45˚ Angle, (B) Fault Direction

Referring to the distance between electrodes, the geometry factor in the Wenner configuration can be formulated as follows:

$$K = 2\pi\alpha$$

So that the apparent resistivity value is obtained:

$$\rho_a = K\frac{\Delta V}{I}$$

2. Research Methods

The specific resistance geoelectric method is one of the techniques in the field of geophysics that examines conditions under the earth's surface by analyzing variations in the distribution of its specific resistance. In this study, the specific gravity geoelectric method is used to investigate the presence of a fault. The faults in question are normal faults and thrust faults. The analysis is conducted through experimental methods. The experimental method is carried out through direct measurements on a fault model made on a laboratory scale.

3. Results And Discussion

From the results of data processing based on the specific resistance value of each measurement path using Res2dinv 3.53 *software*. The material layer in the 2D cross section has a *range of specific* resistance values shown in Table 1.

Table 1. Material Layer

No.	Fault Model	Electrical Resistivity (Ωm)	Materials
1	Normal	± 9,51 - 309	Sandy clay (dry)
		± 309-2254,26	Granite (dry)
2	Up	± 12,51-100	Sandy clay (dry)
		± 100-467,26	Granite (dry)

The normal fault model with a specific resistance value of <309 Ωm is shown with a yellow layer representing a passive clay layer, while a layer with a specific resistance value between 309 and 2254.26 Ωm is shown in red, representing a granite layer. It can be seen that when the measurement is carried out with dry material conditions, the maximum specific resistance value obtained reaches 2254.26 Ωm.

The ascending fault model with a specific resistance value of <100 Ωm is shown with a yellow layer indicating a passive clay layer, while a layer with a specific resistance value between 100 and 467.26 Ωm is shown in red, which is a granite layer. It can be seen that when the measurement is carried out with wet material conditions, the maximum specific resistance value obtained reaches 477.26 Ωm, which is much lower. Compared to dry material. Interpretation of the 2D cross-sectional modeling of type resistance is as follows:

L1 normal cesarean

Based on (Figure 3) in the north-to-south direction (L1) parallel to the fault model, the 2D cross section shows a discontinuous material layer. The 2D cross section shows the significance between the 2D cross section and the fault model, although it is slightly undulated in the material layer. From the interpretation of the figure, the type of obstacles obtained should be expected to follow the description of the rectangular fault model, but in reality, it is not, although in general it is said to be the same. From this case, it can be seen that the geometry model of the fault type resistance does not follow exactly the straight line as in the fault model, but has a slight undulation in the 2D cross-section.

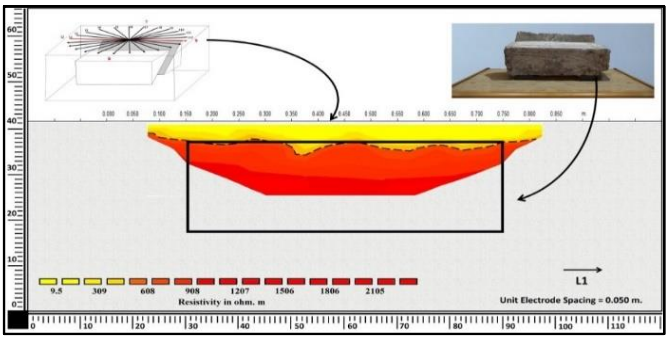

Fig 3. 2D Type Resistance Cross-Section L1 Normal Fault

L5 normal cesarean

Based on (Figure 4) in the northeast-to-west direction (L5) almost perpendicular to the fault model, the 2D cross section shows separate granitic material in the passive clay layer seen between electrodes 4 and 7. The material should decrease towards the west instead of decreasing towards the northeast, it does not yet describe the fault model. From this case, it can be seen that in this direction, the geometry model of the fault type obstacle does not follow exactly as in the fault model, and does not yet describe the fault model. This may be due to the less thorough data collection process.

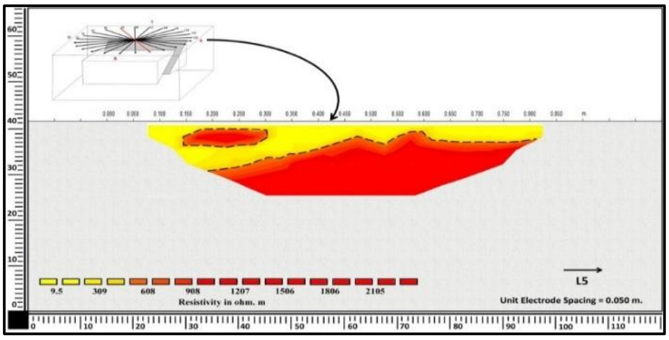

Fig 4. 2D Cross-Section Of L5 Normal Fault Type Resistance

L7 normal cesarean

Based on (Figure 5) in the east-to-west direction (L7) perpendicular to the fault, there is a decrease in the layer of material corresponding to the fault model. The 2D cross section shows a decrease in the passive clay material. From the interpretation of the figure, the cross-section of the normal fault model looks the same, characterized by the sandy clay material that has decreased as the *moving* plane moves down relative to the stationary plane. The straightness of the fault model based on the cross-section of the specific resistance can be determined, namely: Average *strike*: 180˚, average *dip*: 28˚, average *rake*: -28˚, average *trend*: 270˚, and average *plunge*: 45˚. So when taking measurements in the field and the cross-section obtained as in the picture, it can be confirmed that the object is a normal fault.

Tadulako Science and Technology Journal
Vol 1, No. 2, 2021, pp. 1-8
e-ISSN 2776-4893

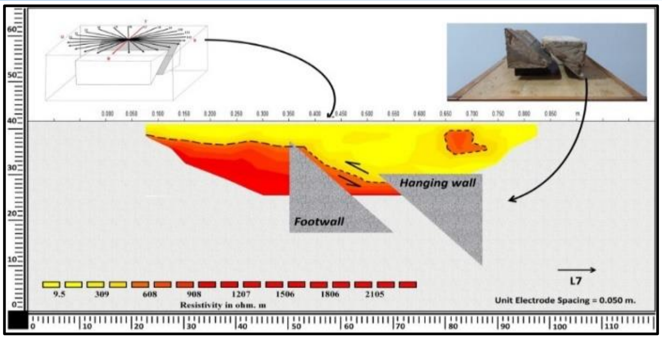

Fig 5. 2D Cross-Section Of L7 Normal Fault Type Resistance

L1 ascending fault

Based on (Figure 6) in the north-to-south direction (L1) parallel to the fault, there are discontinuities in the material layer. The 2D cross section shows irregularities between the passive clay material and granite. From this interpretation, the type of obstacle model obtained should be expected to follow the description of the rectangular fault model, but in reality, it does not, although it is generally said to be the same. From this case, it can be seen that the geometry of the fault-type resistance model does not follow exactly a straight line as in the fault model, but has discontinuities and irregularities between material layers. Therefore, when field measurements are taken and the cross-section obtained is as shown in the figure, it can be confirmed that the object is an ascending fault.

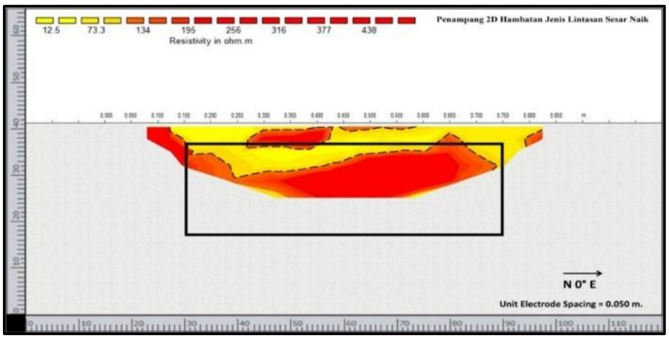

Fig 6. 2D Cross Section Of Type Resistance At L1 Rising Fault

L4 ascending fault

Based on (Figure 7) in the northeast to southwest direction (L4), there is an intersection of material layers. The 2D cross section shows a cut granite layer, visible between electrode stakes 11 to 19. From the interpretation of the figure, the type of obstacle model obtained does not follow the description of the fault model but has an intersection of material in the middle of the material layer. From this case, it can be seen that the geometry model of the fault type resistance does not follow the fault model exactly, but the material layer is cut in the 2D cross-section, which does not reflect the fault model.

Tadulako Science and Technology Journal
Vol 1, No. 2, 2021, pp. 1-8
e-ISSN 2776-4893

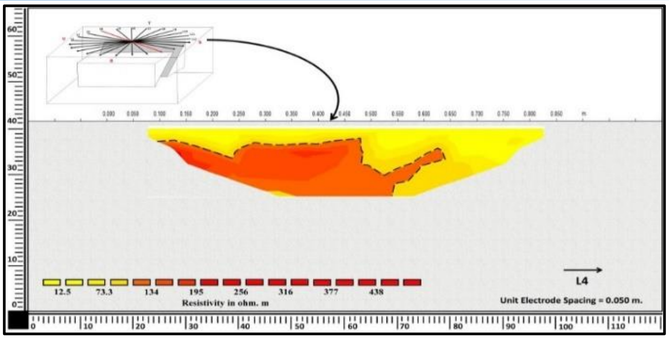

Fig 7. 2D Cross Section Of Type Resistance At L4 Of The Rising Fault

L7 ascending fault

Based on Figure 4.10, in the east-to-west direction (L7) perpendicular to the fault, there is a buildup of granite layers in the center of the cross-section of the fault model. The 2D cross section shows the buildup and tabulation between granites in the (L7) direction. From the interpretation of the image, the The geometry of the cross-section of the type resistance of the rising fault model is similar, marked by the accumulation of granite layers in the center, but the cavity in the model is not detected as the *moving* plane should move up relative to the stationary plane. The straightness of the fault model based on the cross-section of the specific resistance can be determined, namely: *Strike* average: N 180˚ E, average *dip*: 45˚, average *rake*: 45˚, average *trend*: N 270˚ E, and average *plunge*: 45˚ So when taking measurements in the field and the cross-section obtained as in the picture, it can be confirmed that the object is a rising fault.

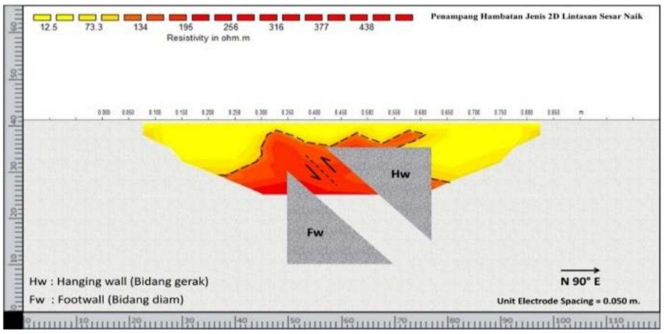

Fig 8. 2D Cross Section Of Type Resistance At L7 Rising Fault

L10 rising fault

Based on Figure 4.11 in the direction of southeast to northwest (L10), it can be seen that there is a discontinuity (discontinuity) in the material layer. The 2D cross-section shows undulations between the passive clay material and granite in the center of the cross-section. From the interpretation of the figure, the type of obstacle model obtained does not follow the description of the fault model but undulates the material in the middle of the material layer.

From this case, it can be seen that the geometry of the fault-type obstacle model does not follow exactly the straight line as in the fault model, but experiences a slight undulation in the 2D cross-section, due to the lack of accuracy in data collection. Of all the 2D cross-sections of the measured obstacles, the cross-sections that are more suitable or have similarities with the model are in the parallel direction and perpendicular direction of the fault model.

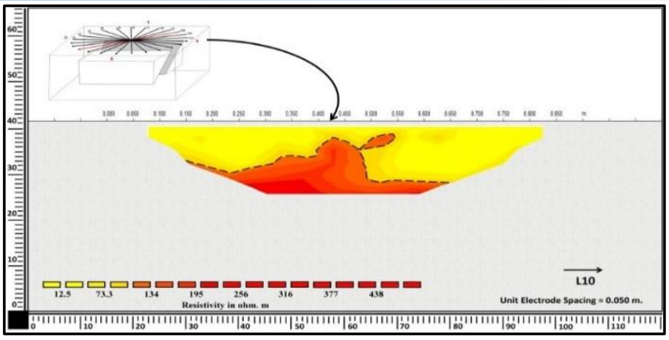

Fig 9. 2D Cross Section Of Type Resistance At L10 Rising Fault

4. Conclusions

Based on the findings and analysis conducted in the laboratory experiments, conclusions can be drawn In testing the effectiveness of the geoelectric method of type resistance, the results obtained show that the effectiveness of the geoelectric method in identifying fault type resistance is more suitable for measurements in the parallel direction and perpendicular direction of the fault model. The fault geometry modeling results show that the normal fault model has a specific resistance value between 309 and 2254.26 Ωm, while the rising fault model has a specific resistance value between 100 and 467.26 Ωm. Both models indicate that the layer is a granitic layer.

References

[1] [PusGeN]. (2017). Indonesia Earthquake Hazard and Source Map. National Earthquake Study Center Team

[2] Abdullah. (2017). Application of Gradient Gravity Method and 2-D Model Analysis of Palu-Koro Fault Structure and Janedo Fault, Donggala-Central Sulawesi. *Thesis*. Postgraduate Applied Geophysics. Bandung Institute of Technology. Bandung.

[3] Ben A. Van Der Pluijm, Stephen Marshak. (2004). *Earth Structure*. Second Edition. University of Michigan.

[4] Billings, M.P., (1959). Structural Geology, New Jersey, Prentice Hall, Inc, Englewood Cliffs.

[5] Gok, R. (2008). Earthquake Focal Mechanism and Waveform Modeling. In *RELEMR Workshop Istanbul*.

[6] Hakim, H., & Manrulu, R. H. (2016). Application of Wenner Configuration in Analyzing Subsurface Material Types. *Scientific Journal of Physics Education Al-Biruni*, 5(1), 95-103.

[7] Marjiyono, M., Kusumawardhani, H., & Soehaimi, A. (2013). Shallow Subsurface Geological Structure Based on Geoelectric Data Interpretation, Case Study of Palu Koro Fault. *Journal of Geology and Mineral Resources,* 23(1), 39-46.

[8] Noor, D. (2014). *Introduction to Geology*. First Edition. Yogyakarta: Deepublish Publisher.

[9] Pratama, I, W. (2018). The Use of Sandbox Analog Modeling as an Educational Tool for Structural Geology and Tectonics in the Dynamic Geology Laboratory. *Proceeding, 11th National Earth Seminar.* Department of Geological Engineering FT UGM.

[10] Salam, R., & Parnadi, W. W. (2021). Laboratory-scaled Azimut Resistivity Survey for Fracture Detection. In *IOP Conference Series: Earth and Environmental Science*, 873 (1), p. 012079. IOP Publishing, 1-2.

[11] Reynolds, J. M. (2011). *An Introduction to Applied and Environmental Geophysics*. England: John Wiley and Sons.

[12] Rosyidi, S.A.P., Taha, M., Lesmana, S. B., Wintolo, J., & Adi, A. D. (2008). Some lessons from the Yogyakarta earthquake of May 27, 2006. International Conference on Case Histories in Geotechnical Engineering. 32.

[13] Rowland, S. M., Duebendorfer, E. M., & Gates, A. (2021). *Structural Analysis and Synthesis: a laboratory course in structural geology*. United States John Wiley & Sons.

[14] Santoso. D. (2002). *Introduction to Geophysical Engineering*. Bandung: ITB Press.

[15] Soehaimi, A. I., Effendi, Setiawan, J.H. and Supartoyo, (2005). Palolo Earthquake Examination Report, January 24, 2005, *Central Sulawesi, Geological Research and Development Center*.

[16] Subiyanto, Y. D. T. N., Suaidi, D. A., & Latifah, E. (2021). Identification of rock layer structure due to fault (Normal Fault) using geoelectric method. *Journal of MIPA and Learning (JMIPAP), 1*(8), 587-595.

[17] Telford, W., M., Geldard, L., P., and Sheriff, R., E. (1990). *Applied Geophysics.* Second Edition. Cambridge University Press.

[18] Wahyuni (2010). Analysis of Obstacle Analysis of Tilted Layer. *Thesis*. Tadulako University. Physics Study Program, Department of Physics FMIPA, Tadulako University. Palu.